X International Conference on Computational Methods in Marine Engineering
MARINE 2023
J. García-Espinosa, L. González, J.E. Gutiérrez & B. Serván-Camas (Eds)

FEM modeling of the mesoscopic section of a polyamide mooring subrope for floating offshore wind turbine; understand the friction to predict the fatigue life.

L. Civier[1†‡], G. Bles[1*], P. Davies[†] and Y. Marco[1]

[1] IRDL-UMR CNRS 6027, ENSTA Bretagne, 2 Rue François Verny, Brest, 29200, Bretagne, France

[†] IFREMER Centre Bretagne, Marine Structures Laboratory, 29280, Plouzané, France

[‡] France Energies Marines, 525 Av. Alexis de Rochon, Plouzané, 29280, Bretagne, France

[*] Corresponding author: Guilhem Bles, guilhem.bles@ensta-bretagne.fr

ABSTRACT

Polyamide-fiber laid-strand ropes are candidates for the shallow-water mooring lines of the future floating offshore wind turbines. Their mesoscopic scale follows a hierarchical architecture: subrope, strands, rope-yarns, yarns, filaments. Their mechanical behavior is the result of friction between components and the visco-elasto-plastic behavior of the filament material. Under cyclic loading, fatigue damage based on the component frictions occurs and is a matter of concern for a 20-year service life. Friction phenomena at the different scales are difficult to quantify experimentally, so we adopted a modeling approach for understanding the friction behaviour. We applied Charmetant's model for describing the deformations within the subrope at the scales of the strand and rope-yarn. Actually, the subrope will be modelled by the quasi-static FEM as three helical strands in contact with each other. Each strand will be meshed by volumic finite elements; at integration points a user-routine behavior law is implemented. As Charmetant et al. showed, this behavior law will distinguish the friction strain modes from the filament material strain mode within the global deformation gradient undergone by the bundle of rope-yarns. For each of these strain modes, a dedicated and relevant behavior law is proposed. Experimental tests are used to identify the model parameters, while, by using other dedicated experimental results, we can afford to test or validate the model predictions.

Keywords: synthetic rope; FOWT; mesoscopic scale; FEM; finite deformation; hyperelastic.

NOMENCLATURE

$\widetilde{\boldsymbol{C}}$	Right Cauchy-Green second-order strain tensor [-]
$\vec{e_{co}}$	Unit vector in the fiber direction [-]
I_1	First invariant of the right Cauchy-Green strain tensor [-]
I_3	Third invariant of the right Cauchy-Green strain tensor [-]
I_4	Invariant for transverse-isotropic laws [-]
I_5	Invariant for transverse-isotropic laws [-]
I_{comp}	Strain invariant for section compaction (Charmetant's model) [-]
I_{dist}	Strain invariant for section distorsion or shear (Charmetant's model) [-]
I_{dist1}, I_{dist2}	Strain invariants for transverse sliding between fibers [-]
I^P_{dist1}, I^P_{dist2}	Plastic strains for transverse friction between fibers [-]
I_{elong}	Strain invariant for fiber elongation (Charmetant's model) [-]
I_{sh}	Strain invariant for shear along the fiber direction (Charmetant's model) [-]
I_{sh1}, I_{sh2}	Strain invariants for longitudinal sliding between fibers [-]
I^P_{sh1}, I^P_{sh2}	Plastic strains for longitudinal friction between fibers [-]
$\widetilde{\boldsymbol{M_o}}$	Unit second-order tensor of the fiber direction [-]
W	Hyperelastic potential per unit of reference volume [$J\ m^{-3}$]
θ	Temperature [$^\circ K$]
$\rho_o\psi$	Free energy per unit of reference volume [$J\ m^{-3}$]

1. INTRODUCTION

Synthetic ropes are candidates for the mooring lines of floating wind turbine in shallow waters (between 50m and 100m). These ropes are made of polymer filaments twisted together to form yarns, that themselves are braided or twisted for the higher scales. One challenge for the station-keeping mooring system is to find a robust and suitable rope solution approved by certification authorities that endures a service life of 20 years. Among others, two phenomena are involved; the creep elongation (Civier et al., 2022) and the fatigue damage due to large numbers of cyclic loadings (Chevillotte et al., 2020). Mandell (1987) found that the major failure mechanism, during low-load and high-cycle fatigue, is the internal abrasion, while at high loads, creep rupture is a matter of concern.

The monitoring of such synthetic ropes may be developed by implanting an optical fiber or other sensors into the braided or twisted rope. That is to say, in the same path as the one of the polymer filaments or between the twisted strands (MONAMOOR project[1]). Then, some questions arise; will the optical fibers be broken or damaged by the cyclic strains of its compressing environment ? Will the sensor implant increase the risk of damage of the rope ? Will the implanted sensor be damaged by the rope?

Usually, during the first tensile loading cycles of a synthetic rope, a specific elongation occurs that is partly due to the bedding-in of the rope elements (yarns, strands) that find their location and section shape, coming into contact, and reaching a stable tensile state (Weller et al., 2014; Lian et al., 2018; Bain et al., 2020). The intricate visco-elasto-plastic tensile behavior of the polymer filament plays a significant role in this elongation. Because of this phenomenon, during mooring installation an at-sea pretension procedure is often applied, called *bedding-in*, in order to stabilize the rope elongation. The understanding of this phenomenon might avoid this expensive process or ease its specification.

[1]MONAMOOR project: https://www.france-energies-marines.org/en/projects/monamoor/

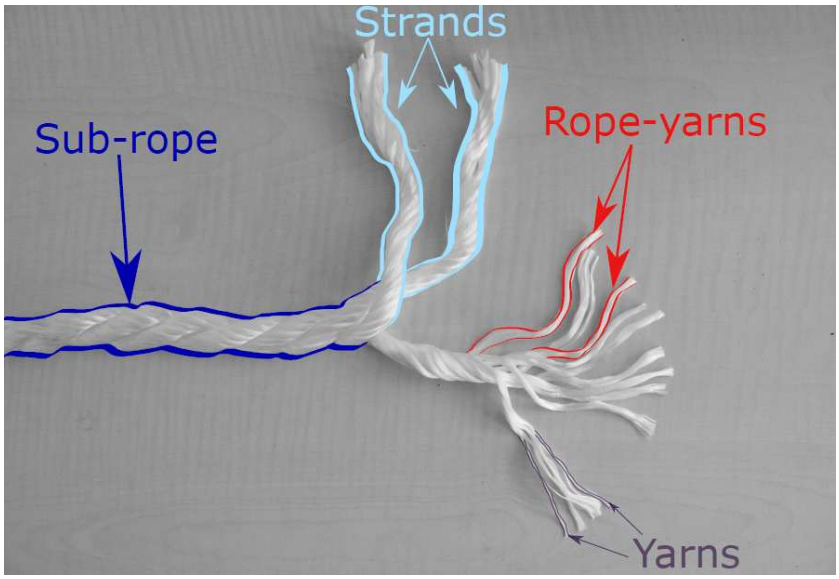

Figure 1: The studied sub-rope and its components at lower scales.

To solve the three major questions listed above an improved understanding of the mechanical phenomena at the scale of the elements of synthetic ropes is required. The mechanics at this scale includes sliding between the yarns, the strands and the associated friction, but also a transverse compression due to the overall rope tension and the helix-shaped paths of the components (Leaf, 1995; Leech, 2002). And always present, the visco-elasto-plastic tensile behavior of the polymer filaments will add its significant contribution.

The present study proposes a way to model the deformation of a synthetic rope at the three higher scales; the sub-rope, the strand and the rope-yarn. The chosen approach is a development of Charmetant's model (Charmetant, Vidal-Sallé and Boisse, 2011). This allows to better understand the mechanics of such ropes at the more impacting scales and an assessment of the dissipated energy due to the internal friction between components and their associated deformation modes.

2. STUDIED SYNTHETIC ROPE

The yarns of the studied rope were supplied by Nexis fibers with a linear weight of 188 tex (g/km) and made of polyamide-6 filaments. The rope is composed of several sub-ropes in parallel. The studied component is these sub-ropes; they are supplied by BEXCO, Hamme Belgium. The linear density of the sub-rope is 90 000 tex (g/km) and their outer diameter is around 12 mm. They are composed of three twisted laid strands. Each strand is composed of twisted rope-yarns, which are themselves composed of yarns. Table 1 and figure 1 describe their hierarchical construction. A proprietary coating was applied on the rope-yarns. To ease mechanical testing on laboratory machines, this studied sub-rope is a reduced-scale model of a polyamide sub-rope developed by Bexco for mooring lines.

3. MODEL

Because of the multi-scale hierarchical construction of synthetic ropes (Tab. 1), the modeling approach has to select how many scales to describe. Table 2 gives some possible approaches. Method A does not assume any simplification. The filaments are modeled by a 1D chain of beam elements. Thus,

Table 1: The hierarchical construction of the synthetic rope.

	Rope	Sub-rope	Strand	Rope-yarn	Yarn	Filament
Scale level	0	1	2	3	4	5
Quantity in the immediate upper scale	/	10 for example	3	10	13	280

Table 2: Different FEM modeling approaches for a sub-rope.

	Sub-rope	Strand	Rope-yarn	Yarn	Filament
Scale level	1	2	3	4	5
Modeling method A	contact between lower-scale elements	contact between lower-scale elements	contact between lower-scale elements	contact between lower-scale elements	1 chain of beam elements
Modeling method B	contact between lower-scale elements	contact between lower-scale elements	1 chain of beam elements	/	/
Modeling method C	contact between lower-scale elements	mesh of 3D solid elements	transverse-isotropic law for a rope-yarn bundle as a homogeneous material	/	/

this model has to deal with the numerous contact possibilities between scale 5 up to scale 1. In this type of model, the contact-pair management is one of the difficult key points (Durville, 2012; Wielhorski and Durville, 2015; Wang et al., 2022). So, method A is probably not achievable. We will therefore reduce the number of modeled scales; this is method B, where each rope-yarn is described by one chain of beam elements. Some authors, like Durville and Wang, managed to deal with this type of model. However, the contact-interaction management remains a challenge, so the tensile behavior of the components is limited; for example elasticity or damaged elasticity.

Another modeling approach that avoids the numerous contact interaction management, is possible. By releasing this difficult point, we aim to be able to implement more realistic behavior laws for the components of synthetic ropes. Indeed, polymer filaments (polyester, polyamide), that constitute mooring synthetic ropes, often have a complex one-dimensional visco-elasto-plastic behavior. We propose to choose method C on table 2 as Charmetant, Vidal-Sallé and Boisse (2011) did in the case of a woven fabric. Each strand will be meshed with three-dimensional solid finite elements (Fig. 2). We consider the strand to be made of a homogeneous material. This reduces greatly the number of contact interactions. Hence, to represent the sub-scale physics at the integration points of the solid elements, a behavior law has to model the transverse-isotropic behavior of the rope-yarn bundle.

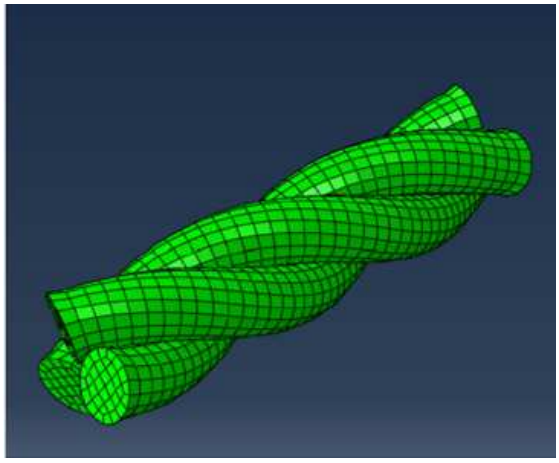

Figure 2: Illustration of a FEM sub-rope model according to method C (Tab. 2).

3.1 Charmetant's model

Charmetant, Vidal-Sallé and Boisse (2011) proposed a relevant behavior law for a glass-fiber bundle. They chose method C to model the behavior of a woven fabric made of glass-fiber yarns. They meshed the yarns with 3D solid elements and considered fiber bundles as a homogeneous material. They proposed the four following strain scalar invariants :

$$I_{comp} = \frac{1}{4}\ln\left(\frac{I_3}{I_4}\right) \qquad I_{elong} = \frac{1}{2}\ln I_4 \tag{1}$$

$$I_{dist} = \frac{1}{2}\ln\left[\frac{I_1 I_4 - I_5}{2\sqrt{I_3 I_4}} + \sqrt{\left(\frac{I_1 I_4 - I_5}{2\sqrt{I_3 I_4}}\right)^2 - 1}\right] \qquad I_{sh} = \sqrt{\frac{I_5}{I_4^2} - 1} \tag{2}$$

with

$$I_1 = \mathrm{Tr}\widetilde{\boldsymbol{C}} \qquad I_3 = \det\widetilde{\boldsymbol{C}} \qquad I_4 = \widetilde{\boldsymbol{C}} : \widetilde{\boldsymbol{M_o}} \qquad I_5 = \left(\widetilde{\boldsymbol{C}} \cdot \widetilde{\boldsymbol{C}}\right) : \widetilde{\boldsymbol{M_o}} \tag{3}$$

$$\widetilde{\boldsymbol{M_o}} = \vec{e}_{co} \otimes \vec{e}_{co} \tag{4}$$

where $\widetilde{\boldsymbol{C}}$ is the right Cauchy-Green strain second-order tensor and $\vec{e}_{co}$ is a unit vector along the direction of the fibers in the reference configuration.

They assumed a hyperelastic behavior law according to the following potential :

$$\rho_o\psi\left(\theta, I_{comp}, I_{elong}, I_{dist}, I_{sh}\right) = W_{comp}(\theta, I_{comp}) + W_{elong}(\theta, I_{elong}) + W_{dist}(\theta, I_{dist}) + W_{sh}(\theta, I_{sh}) \tag{5}$$

where $\rho_o\psi$ is the free energy per unit of reference volume and θ is the temperature.

This allows implementation, for each strain invariant, of a dedicated and relevant behavior law. Each strain invariant captures a strain mode within the deformation gradient of the fiber bundle. All these strain modes together define completely the deformation gradient except for the proper rotation. These strain modes are presented at figure 3. The strain modes I_{comp} and I_{elong} describe the axial tension behavior of the fibers and the volume-change behavior of the fiber bundle. While strain modes I_{dist} and I_{sh} describe the sliding between the fibers with a relative velocity in the transverse direction and the longitudinal direction, respectively.

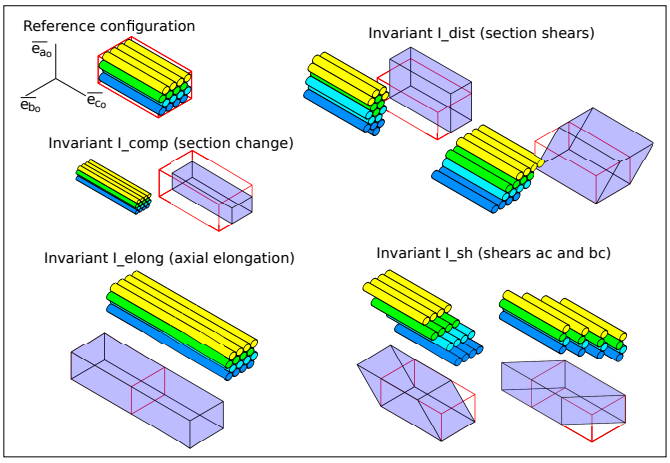

Figure 3: Strain modes of a fiber bundle according to the Charmetant's strain invariants.

3.2 Development of Charmetant's model

But Charmetant, Vidal-Sallé and Boisse (2011) chose only one strain invariant for the transverse sliding, while there are actually two different modes, as illustrated by figure 3. The same remark can be made for the longitudinal sliding. So, we developed Charmetant's model to include two more strain invariants, in order to take into account all the sliding modes :

$$I_{dist} \Longrightarrow (I_{dist1}, I_{dist2}) \qquad I_{sh} \Longrightarrow (I_{sh1}, I_{sh2}) \tag{6}$$

And we defined a hyperelasto-plastic model to describe the friction behaviors of the strain modes (I_{dist1}, I_{dist2}) (transverse friction) and (I_{sh1}, I_{sh2}) (longitudinal friction), as follows :

$$\rho_o \psi = W_A\left(\theta, I_{comp}, I_{elong}\right) + W_{trans}\left(\theta, I_{dist1} - I^P_{dist1}, I_{dist2} - I^P_{dist2}\right) + W_{long}\left(\theta, I_{sh1} - I^P_{sh1}, I_{sh2} - I^P_{sh2}\right) \tag{7}$$

where I^P_{dist1}, I^P_{dist2}, I^P_{sh1} and I^P_{sh2} are plastic strains that describe the sliding when friction occurs.

4. IDENTIFICATION

The identification of the model parameters has to be performed at the scales of the rope-yarn and the strand. A tensile test on a rope-yarn allowed us to identify the hyperelastic potential W_A and its parameters (Fig. 4-left). While a tensile test, where a strand is in contact with a rigid rod, allows us to identify the parameter of potential W_{trans} (Fig. 4-right). A tensile test on a strand will allow us to identify the parameter of potential W_{long}.

5. EXAMPLE OF SIMULATION: BENDING A STRAND

The following is an illustration of achievable results using this model. A strand, composed of rope-yarns twisted together according to an helix angle of 30° as shown on figure 5, is simulated. The initial or reference configuration is the straight one as on figure 5. The mesh is composed of 2400 three-dimensional 8-node hexahedron linear elements (named *C3D8*). The nodes are not aligned with the rope-yarn axes, but with the strand axis. At each integration point, the behavior law defines the rope-yarn direction by dedicated parameters.

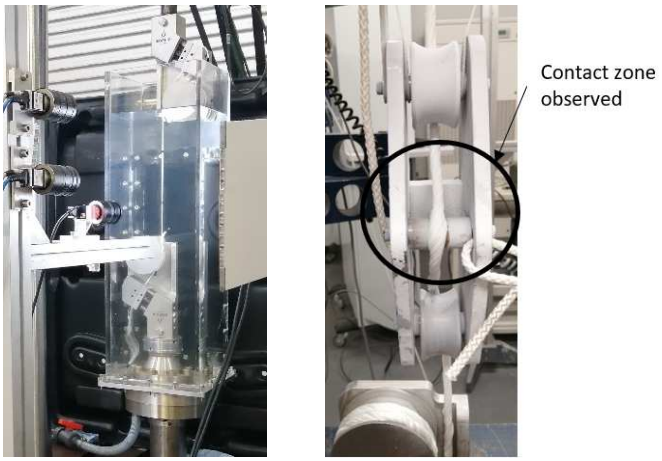

Figure 4: Identification mechanical tests: (left) tensile test on a rope-yarn, (right) contact of a tensile strand on a rod.

The finite element analysis is quasi-static, using a classical Newton-Raphson algorithm to reach the equilibrium node displacement field. The behavior law was implemented into an user-routine (*UMAT*). The finite element code was *Abaqus-Standard*.

We aimed to simulate the bending of the strand; starting with the straight shape; we applied symmetric rotation on both extremities to reach an arc shape (half of a circle). The boundary conditions are described on figure 6.

The resulting deformation of the strand is given on figure 7. We expected the shape to be a half-circle, but the behavior of the strand resulted in a different shape, where a high bending curvature is localized between two symmetric sections. Also, the strand did not stay in the plane $Y - Z$. The initial section shape was circular, while, after bending, in the high-curvature areas, the section shape has changed significantly.

The dissipated energies due to the two friction modes, *transverse* and *longitudinal*, are given on figures 8 and 9, respectively. We observe that the two frictions do not occur at the same location of the bent area. The tranverse friction appears more on the external side of the curvature, while the longitudinal friction occurs on the internal side. The dissipated-energy density of the longitudinal friction is much higher than the one of the transverse friction, but the former is more localized in a smaller area than the latter.

6. CONCLUSION

We developed the model of Charmetant, Vidal-Sallé and Boisse (2011) for taking into account the friction between the components of a synthetic rope. Indeed, Charmetant proposed a hyperelastic model that is not compatible with a friction model, so we added two more strain invariants to be able to model the frictions between the fibers. A major advantage of Charmetant's approach is to be able to apply relevant behavior laws for each strain mode of a fiber bundle. Notably, the friction are modeled by a shear strain and two modes are distinguished; the transverse friction between the fibers and the longitudinal one. Elasto-plastic laws were chosen to model these frictions. We applied this enhanced approach to the strand that composed a sub-rope of a FOWT mooring line. Once this model has been fully identified and validated, we will be able to predict the frictions between the three strands and also between the rope-yarns inside the strands, their dissipated energies and all

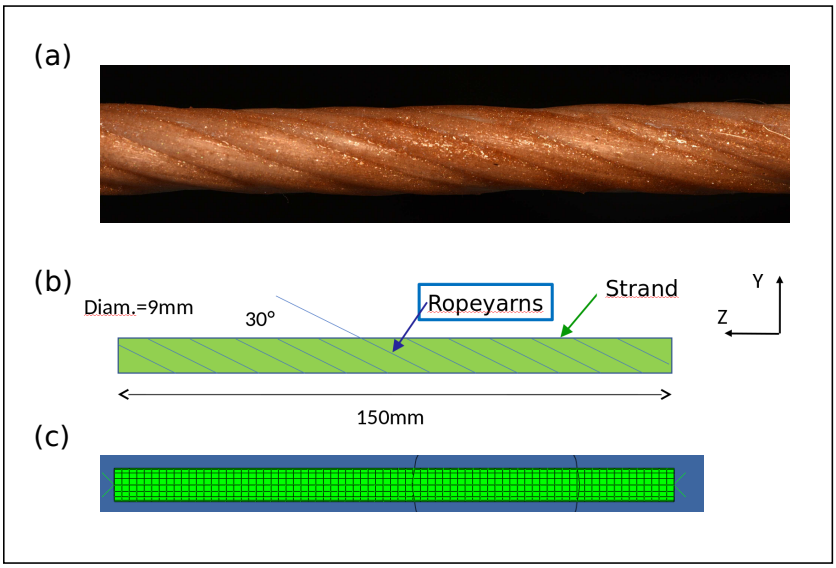

Figure 5: The simulated strand: (a) a picture of a sub-rope strand, (b) its dimensions and (c) the 2400-element mesh.

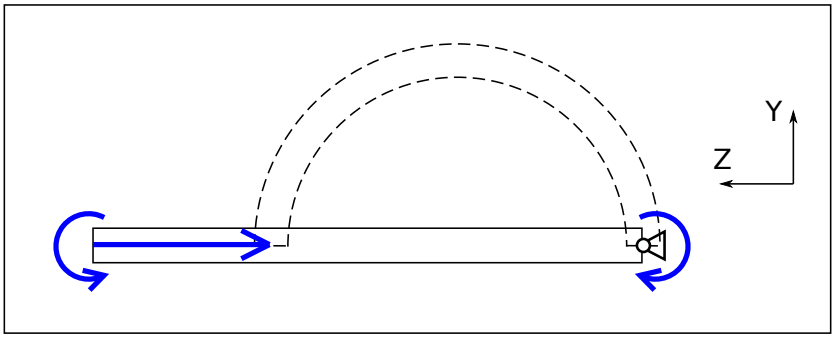

Figure 6: Boundary conditions applied to the strand for the bending simulation: the blue arrows specify the imposed displacement and rotations. The dashed lines describe the a-priori expected bent configuration. The two-rotation angles are $\pm\frac{\pi}{2}$.

deformation within the sub-rope. This model will be a helpful numerical tool to better understand the fatigue performance, the impact of sensors implanted within the sub-rope, and the deformation and elongation that occur during the bedding-in of synthetic fibre ropes.

ACKNOWLEDGEMENTS

This work is performed within the MONAMOOR project, that receives funding from France Energies Marines and its members and partners, as well as French State funding managed by the National Research Agency under the France 2030[2] investment plan (ANR-10-IEED-06-34). This project is led by France Energies Marines with partners Saipem, Bureau Veritas, BEXCO Ropes, ENSTA Bretagne, IFREMER, Naval Energies, Total Energies, University of Nantes, University Gustave Eiffel, NCD,

[2]Funded by

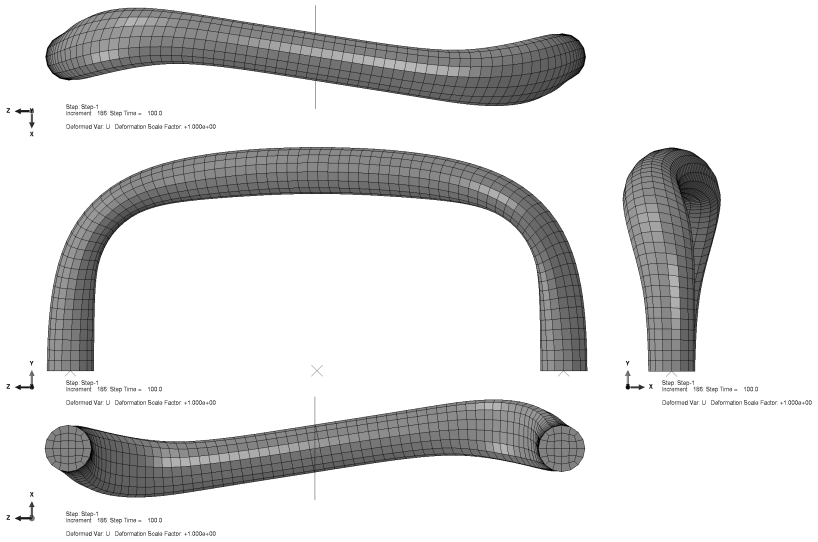

Figure 7: Deformation of the bent strand resulting from boundary conditions of figure 6.

IFSTTAR, GeM, CNRS, WEAMEC and RWE.

REFERENCES

References

Bain, C., Davies, P., Bles, G., Marco, Y. and Barnet, J., 2020. Influence of bedding-in on the tensile performance of hmpe fiber ropes. *Ocean Engineering*, 203, p.107144.

Charmetant, A., Vidal-Sallé, E. and Boisse, P., 2011. Hyperelastic modelling for mesoscopic analyses of composite reinforcements. *Composites Science and Technology*, 71, pp.1623–1631.

Chevillotte, Y., Marco, Y., Bles, G., Devos, K., Keryer, M., Arhant, M. and Davies, P., 2020. Fatigue of improved polyamide mooring ropes for floating wind turbines. *Ocean Engineering*, 199, p.107011.

Civier, L., Chevillotte, Y., Bles, G., Montel, F., Davies, P. and Marco, Y., 2022. Short and long term creep behaviour of polyamide ropes for mooring applications. *Ocean Engineering*, 259, p.111800.

Durville, D., 2012. Contact-friction modeling within elastic beam assemblies: an application to knot tightening. *Comput Mech*, 49, pp.687–707.

Leaf, G., 1995. The friction couple in yarn bending. *The Journal of The Textile Institute*, 86(1), pp.45–54.

Leech, C., 2002. The modelling of friction in polymer fibre ropes. *International Journal of Mechanical Sciences*, 44, pp.621–643.

Lian, Y., Liu, H., Li, L. and Zhang, Y., 2018. An experimental investigation on the bedding-in behavior of synthetic fiber ropes. *Ocean Engineering*, 160, pp.368–381.

Mandell, J.F., 1987. Modeling of marine rope fatigue behavior. *Textile Research Journal*, 57(6), pp.318–330.

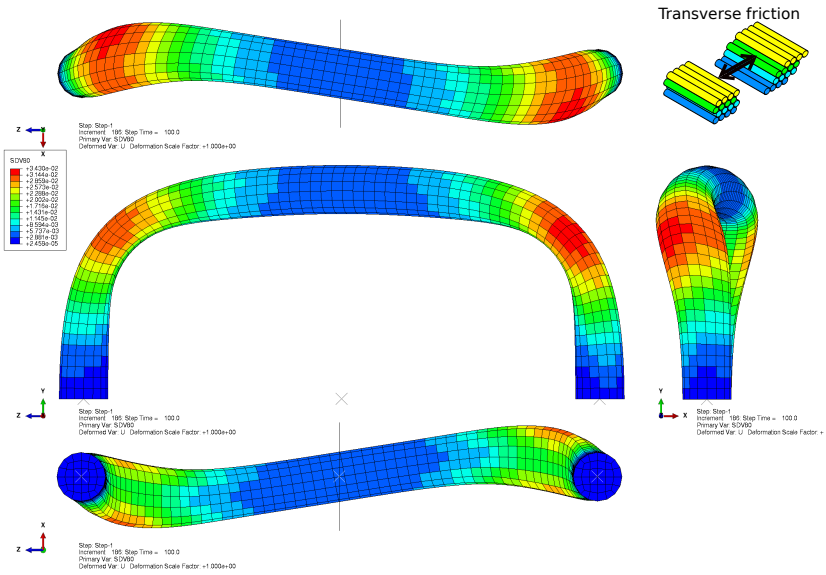

Figure 8: Dissipated energy of the bent strand resulting from boundary conditions of figure 6: dissipated energy for the **transverse friction mode** between the rope-yarns, per unit of reference volume. The unit is $mJ\ mm^{-3}$.

Wang, Y., Jiao, Y., Wu, N., Xie, J., Chen, L. and Wang, P., 2022. An efficient virtual modeling regard to the axial tensile and transverse compressive behaviors of the twisted yarns. *Journal of Industrial Textiles*, 52, p.15280837221137353.

Weller, S., Davies, P., Vickers, A. and Johanning, L., 2014. Synthetic rope responses in the context of load history: Operational performance. *Ocean Engineering*, 83, pp.111–124.

Wielhorski, Y. and Durville, D., 2015. Finite element simulation of a 3d woven fabric: determination of the initial configuration and characterization of the mechanical behavior. *Texcomp-12 conference*.

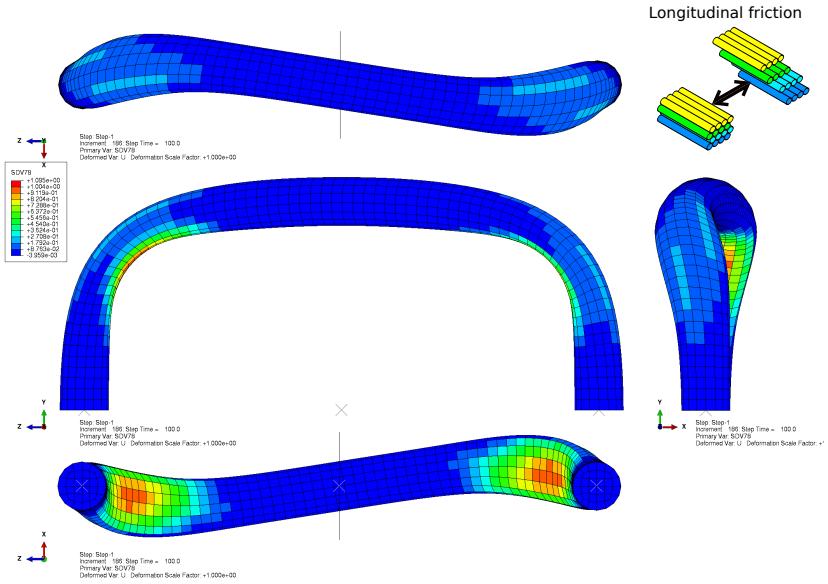

Figure 9: Dissipated energy of the bent strand resulting from boundary conditions of figure 6: dissipated energy for the **longitudinal friction mode** between the rope-yarns, per unit of reference volume. The unit is $mJ\ mm^{-3}$.